Korean J. Chem. Eng., 40(2), 436-444 (2023)
DOI: 10.1007/s11814-022-1298-6

pISSN: 0256-1115
eISSN: 1975-7220

Patterning potential of the terminal system in the *Drosophila* embryo

Keonyong Lee*,‡, Kate Molloy O'Neill,***,‡, Jayoung Ku*, Stanislav Yefimovic Shvartsman****,*****,******, and Yoosik Kim*,†**

*Department of Chemical and Biomolecular Engineering, Korea Advanced Institute of Science and Technology (KAIST), Daejeon 34141, Korea
**Institute for Physical Science and Technology, University of Maryland, College Park, MD 20742, United States
***Department of Chemical and Biological Engineering, Princeton University, Princeton, NJ 08540, United States
****Lewis Sigler Institute for Integrative Genomics, Princeton University, Princeton, NJ 08540, United States
*****Center for Computational Biology, Flatiron Institute, Simon Foundation, New York, NY 10010, United States
******Department of Molecular Biology, Princeton University, Princeton, NJ 08540, United States
(*Received 8 August 2022 • Revised 17 September 2022 • Accepted 23 September 2022*)

Abstract−Segmentation of the *Drosophila* embryo is initiated by localized maternal signals. In this context, anteriorly localized Bicoid activates the gap genes in the anterior half of the embryo while posteriorly localized Nanos represses the translation of maternal *hunchback* mRNA to pattern the posterior half. The non-segmented termini are patterned by the localized activation of mitogen-activated protein kinase. Yet, the spatial extent of the terminal patterning system in regulating gap genes beyond poles remains unknown. We investigated the patterning potential of the terminal system using mutagenized embryos that lack both the anterior and the posterior maternal signaling systems. Using a combination of quantitative imaging and mathematical modeling, we analyzed the spatial patterns of gap genes in the early *Drosophila* embryo. We found that this mutant embryo develops symmetric cuticle patterns along the anteroposterior axis with two segments on each side. Notably, the terminal system can affect the expression of *Krüppel* in the torso region. Our mathematical model recapitulates the experimental data and reveals the potential bistability in the terminal patterning system. Collectively, our study suggests that the terminal system can act as a long-range inductive signal and establish multiple gene expression boundaries along the anteroposterior axis of the developing embryo.

Keywords: Signal Transduction, Embryogenesis, MAPK, Gap Genes, Bistability

INTRODUCTION

Segmentation during embryogenesis is essential to ensure proper cell fate determination and development of body parts. In the *Drosophila* embryo, segmentation occurs in a series of steps, as summarized in Fig. 1(a) [1,2]. First, the body axes of the embryo are set up by the maternal genes, and broad regional differences are established by the gap genes [3-6]. These differences are further refined by the pair-rule genes, segment polarity genes, and homeotic selector genes [7]. These genes pattern themselves into stripes and eventually result in the segmentation of the larvae, which can be visualized through cuticles of the first instar larvae of Oregon R (OreR) wild-type flies (Fig. 1(b)).

Patterning of the anteroposterior (AP) axis of the *Drosophila* embryo is initiated by three localized maternal signals: the anterior, posterior, and terminal systems. In the anterior region, maternally deposited *bicoid* (*bcd*) mRNA generates a gradient of Bcd protein, which then works as a morphogen to activate a group of genes required for head patterning [8]. Indeed, the cuticle of embryos without *bcd* lacks the entire head structure (Fig. 1(c)). Bcd also represses the translation of *caudal* mRNAs to limit their protein expression to the posterior half [9,10]. Together with posteriorly localized Nanos, Caudal patterns the posterior region of the embryo [11,12]. Nanos also represses the translation of maternally deposited *hunchback* (*hb*) mRNA to restrict the expression of maternal Hb protein in the anterior half of the embryo [13].

The terminal regions of the embryo are patterned by a highly conserved mitogen-activated protein kinase/extracellular signal-regulated kinase (MAPK/ERK) signaling pathway, also known as the terminal patterning system [14,15] (Fig. 1(d)). MAPK signaling is activated by local activation of Torso (Tor) receptor tyrosine kinase by the localized processing of its ligand trunk (Trk) [16]. Activated Tor then signals through conventional MAPK signaling cascade, which results in the double-phosphorylation of MAPK, encoded by the gene *rolled* in *Drosophila*. Phosphorylated MAPK, also known as dpERK, then allows terminal gap genes *tailless* (*tll*) and *huckebein* (*hkb*) to be derepressed by phosphorylating a number of translational repressors, including Capicua (Cic) and Groucho (Gro) [17,18]. Through examination of cuticles from embryos lacking components of the terminal system, it has been established that the terminal system is required to pattern the terminal non-segmented regions of the embryo (Fig. 1(e)).

Traditionally, the terminal patterning system is required to pattern the poles of the embryo. However, quantification of the gradients of dpERK and its substrate Cic in wild-type embryos revealed

†To whom correspondence should be addressed.
E-mail: ysyoosik@kaist.ac.kr
‡These authors contributed equally.

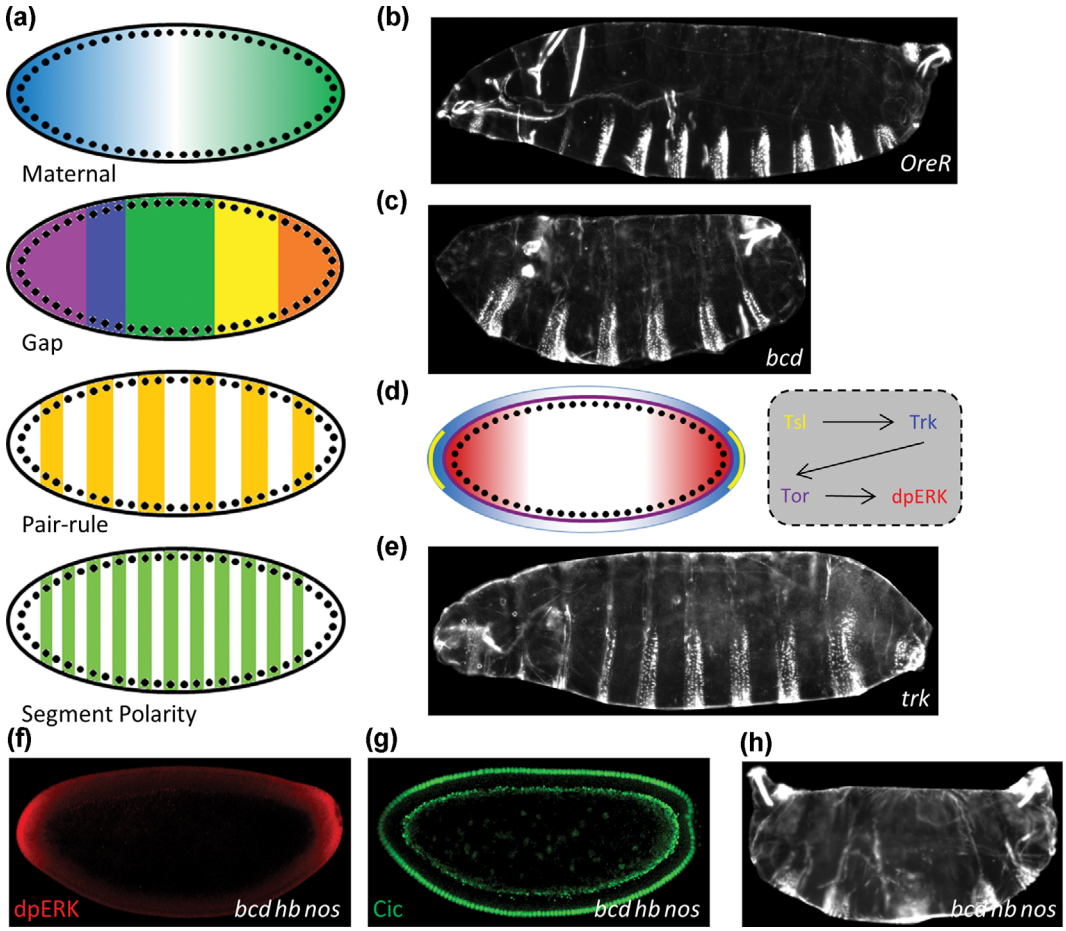

Fig. 1. Patterning of the early *Drosophila* embryo by maternal signaling systems. (a) Schematic of the segmentation process during *Drosophila* embryogenesis. (b) First instar larval cuticle of wild-type OreR embryos. (c) Embryonic cuticle produced by embryos lacking *bcd*. (d) Schematic of the spatial distribution of components of the terminal patterning system. (e) Embryonic cuticle produced by embryos lacking Tor ligand *trk*. (f), (g) Immunostaining of dpERK (f) and Cic (f) in *bcd hb nos* germline clone embryos. (h) Embryonic cuticle by embryos lacking *bcd*, maternal *hb*, and *nos*.

that they are surprisingly shallow, especially in the posterior half of the embryo [19]. Moreover, a recent study using an optogenetic system to control MAPK revealed that the ectopic activation of MAPK resulted in derepression of the terminal gap genes throughout the embryos, resulting in embryos lacking segments [20]. Clearly, when activated, the terminal patterning system has the potential to regulate gene expression beyond just the terminal region of the embryo. Yet, it is unclear whether the terminal system is responsible for patterning only the last segment or whether it can serve as a morphogenic signal to generate multiple segments.

In this study, we used mutant embryos that lack both the anterior and the posterior maternal signaling systems to investigate the spatial extent of the terminal system in patterning the AP axis of the embryo. We analyzed the gap gene expression patterns and the formation of cuticle structures in these embryos to examine whether the terminal system could affect the gene expression in the torso region and generate multiple segments. Moreover, we generated mutant embryos that retained maternal *hb*, but lacked *bcd* and *nos*, to examine whether maternal Hb plays a role in regulating the spatial range of the terminal system. Lastly, we employed mathematical modeling of the gap gene regulation by the terminal system to analyze the potential existence of bistability in the system. Collectively, our study reveals the spatial extent of the terminal system in patterning the *Drosophila* embryo and provides the potential function of maternal Hb protein in regulating the spatial range of the terminal system.

MATERIALS AND METHODS

1. Fly Strains

The following fly strains were used in this study: *OreR, FRT82B-hb[FB]-nos[BN]-bcd[E1], nos[BN]-bcd[E1], trk[1], bcd[E1],* and *tor[4021].*

2. Cuticle Preparation

Embryos were harvested 24 h after egg laying and dechorionated in 50% bleach. Dechorionated embryos were incubated in a 1 : 4 mixture of glycerol : acetic acid for 1 h at 65 °C, mounted on a slide, and kept at 65 °C overnight before imaging.

3. RNA Fluorescent In Situ Hybridization (RNA-FISH)

Embryos were harvested 4 h after egg laying, dechorionated in

50% bleach for 1 min, fixed in 8% formaldehyde for 20 min, and devitellinized in methanol with vigorous shaking. Fixed embryos were treated with a 9 : 1 mixture of xylene and ethanol for 1 h and washed three times with ethanol and three times with methanol. Embryos were post-fixed in a 1 : 1 mixture of methanol : 5% formaldehyde in phosphate-buffered saline supplemented with 0.02% Triton X-100 (PBST) for 5 min. Post-fixed embryos were then incubated with 80% acetone for 10 min at −20 °C and washed with PBST three times. Embryos were post-fixed for the second time in 5% formaldehyde in PBST for 25 min. Fixed embryos were incubated with hybridization buffer at 60 °C for 2 h.

Embryos were then hybridized overnight at 60 °C with antisense probes labeled with digoxigenin (DIG), biotin (BIO), or fluorescein (FITC). After hybridization, embryos were washed with pre-warmed hybridization buffer every 45-60 min for 3-4 h. Embryos were washed three times with PBST and blocked in 20% Western Blocking Reagent (WBR) for 30 min. Embryos were incubated in primary antibodies diluted in 20% WBR overnight at 4 °C. Embryos were washed three times with PBST and incubated with secondary antibodies in 20% WBR for 90 min at room temperature. Embryos were washed three times with PBST and mounted on a microscope slide for imaging. The following antibodies were used in this study: sheep anti-DIG (Roche, 1 : 200), mouse anti-BIO (Jackson ImmunoResearch, 1 : 200), rabbit anti-FITC (Thermo Fisher Scientific, 1 : 200), and Alexa fluor conjugated secondary antibodies (Thermo Fisher Scientific, 1 : 500). DAPI (Vector Laboratories, 1 : 10,000) was used to detect nuclei. Images of the nuclei on the surface were analyzed to determine embryos in the cell cycle 14 stage as described elsewhere [21].

4. Immunostaining

Devitellinized embryos fixed in 8% formaldehyde were blocked in 10% bovine serum albumin (BSA) and 5% normal goat serum (NGS) in PBST overnight at 4 °C. Embryos were rinsed with PBST and incubated in primary antibodies diluted in 1% BSA and 5% NGS for 3 h at room temperature. Embryos were washed three times with PBST and incubated with Alexa fluor conjugated secondary antibodies diluted in 1% BSA and 10% NGS solution for 90 min at room temperature. Embryos were stained with DAPI and mounted on a microscope slide for imaging. The following antibodies were used in this study: mouse anti-dpERK (Sigma-Aldrich, 1 : 100), anti-Cic (a gift from G. Jimenez, 1 : 2,000), and Alexa fluor conjugated secondary antibodies (Thermo Fisher Scientific, 1 : 500). DAPI was used to counterstain the nuclei, which were then used to determine cell cycle 14 embryos.

5. Microscopy and Image Processing

Imaging was done on a Zeiss LSM510 confocal microscope with Zeiss C-Apo 20x (NA=0.6) objective. Images were obtained from a focal plane on the surface of the embryo for RNA-FISH and on the center of the embryo for immunostaining. Images of individual embryos were automatically extracted from raw confocal files and re-oriented and processed as described elsewhere [21].

6. Quantification of Gene Expression Boundaries

The expression boundaries of the gap genes were determined using an automated image analysis program in Matlab [22]. Briefly, the program finds the boundary of the embryo and averages staining intensity along the dorsoventral axis. This was performed for 1,000 points uniformly spaced along the AP axis, generating an AP expression profile of the gene. The data were then normalized by dividing them by the maximum intensity. The inflection point was used as a boundary of the gene expression domain.

7. Mathematical Model

The spatial gradient of dpERK was estimated by applying the image processing analysis [21]. This experimental data was used to determine parameters for the dpERK gradient, which was estimated as the sum of two Gaussian distributions centered at the anterior and posterior poles. To model the Cic gradient, the Michaelis-Menten equation was applied using dpERK as the spatial concentration gradient for the enzyme.

The gap genes were modeled using the reaction and diffusion equation:

$$\frac{\partial C_i}{\partial t} = D\frac{\partial^2 C_i}{\partial x^2} - k_{d_i} C_i + A_i S(C)$$

where

C_i is the concentration of the gene i
D is the diffusivity
k_{d_i} is the degradation rate for the gene i
A_i is the rate of transcription of the gene i
S(C) is the Heaviside step function for the gene transcription

The Heaviside step function was designed to compare the transcription activation threshold for gene *i* to the strength of the genes repressing it.

$$S(C)=H(\theta_i - W * C)$$

where

θ_i is the activation threshold for the gene i
W is the 6x6 matrix for the repressive weights

For *tll* and *hkb*, a slightly different expression was used to allow gene depression by Cic downregulation.

$$S(C)=H(\theta_i - C_{Cic})$$

where

C_{Cic} is the concentration of Cic protein along the AP axis.

The resulting mathematical model was analyzed using Matlab.

RESULTS AND DISCUSSION

1. The Terminal System Alone Can Generate Multiple Segments Along the AP Axis

To investigate the patterning potential of the terminal system, we generated germline clone embryos that lack *bcd*, maternal *hb*, and *nos* (denoted as *bcd hb nos*). We first confirmed that these embryos still possess a functional terminal patterning system by visualizing the dpERK activation at the poles, which subsequently resulted in the downregulation of Cic in these regions (Figs. 1(f) and 1(g)). We then analyzed the cuticle of this mutant embryo and found that the embryo developed into a symmetrical pattern with a total of five segments (Fig. 1(h)). This indicates that the terminal system alone is capable of generating multiple segments well into the torso region of the embryo.

2. Analysis of the Gap Gene Expression Patterns in OreR and *bcd hb nos* Mutant Embryos

We then employed RNA-FISH to analyze the gap gene expression patterns in this mutant background. Previously established regulation among the gap genes is summarized in Fig. 2(a) [23,24]. We first confirmed the validity of our RNA-FISH probes using OreR wild-type embryos which reproduced previously established gap gene patterns (Fig. 2(b)). Of note, all images were obtained from embryos in cell cycle 14, which was determined by analyzing the number of nuclei visualized through DAPI staining. We further quantified the fluorescence signal intensity and used the inflection point to infer the expression boundary of the genes (Fig. 2(c)). Our

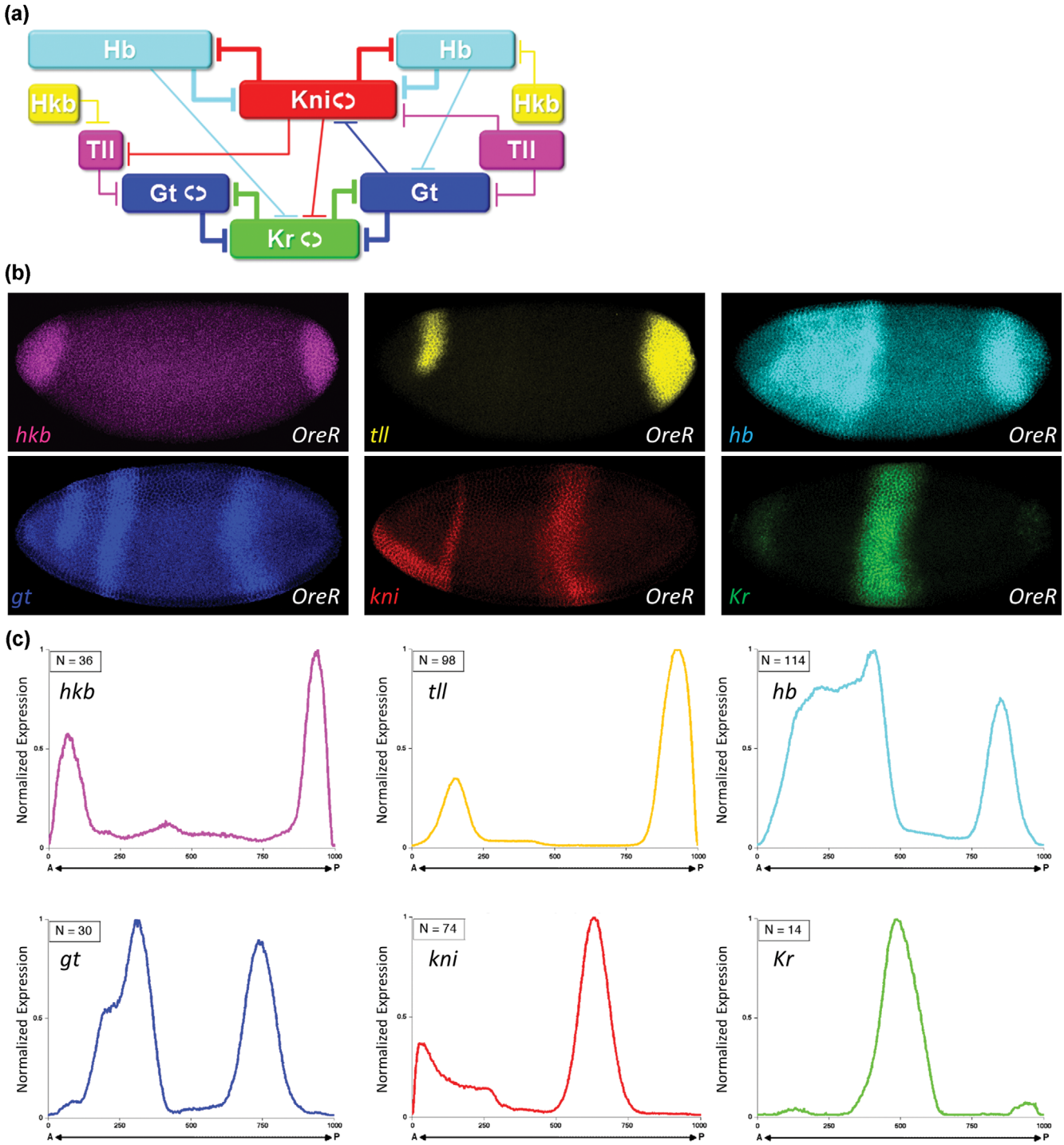

Fig. 2. Gap gene expression patterns in wild-type embryos. (a) Schematic of the expression and regulatory model of the gap genes based on previous studies. (b) RNA-FISH image of the six gap genes in wild-type embryos. (c) Quantified expression profiles of the gap genes in wild-type embryos. Average profiles are shown with the number of embryos indicated in each plot.

results were consistent with the previous data reported by Ashyraliyev and colleagues [23].

The gap gene network is dominated by mutually repressive relationships, which are easily observed by comparing the quantified gene expression patterns. We first smoothed the average gene expression data to reduce noise. Consistent with the previous relationships, *Krüppel* (*Kr*) and *giant* (*gt*) as well as *knirps* (*kni*) and zygotic *hb* showed very strong mutually repressive relationships. In addition, *hb* and *hkb* as well as *Kr* and *kni* showed weak repressive relationships. However, in our data, *gt* and *hb* did not show a strong repressive relationship, and we also did not observe repressive interaction between *kni* and *gt* as these genes were expressed in over-

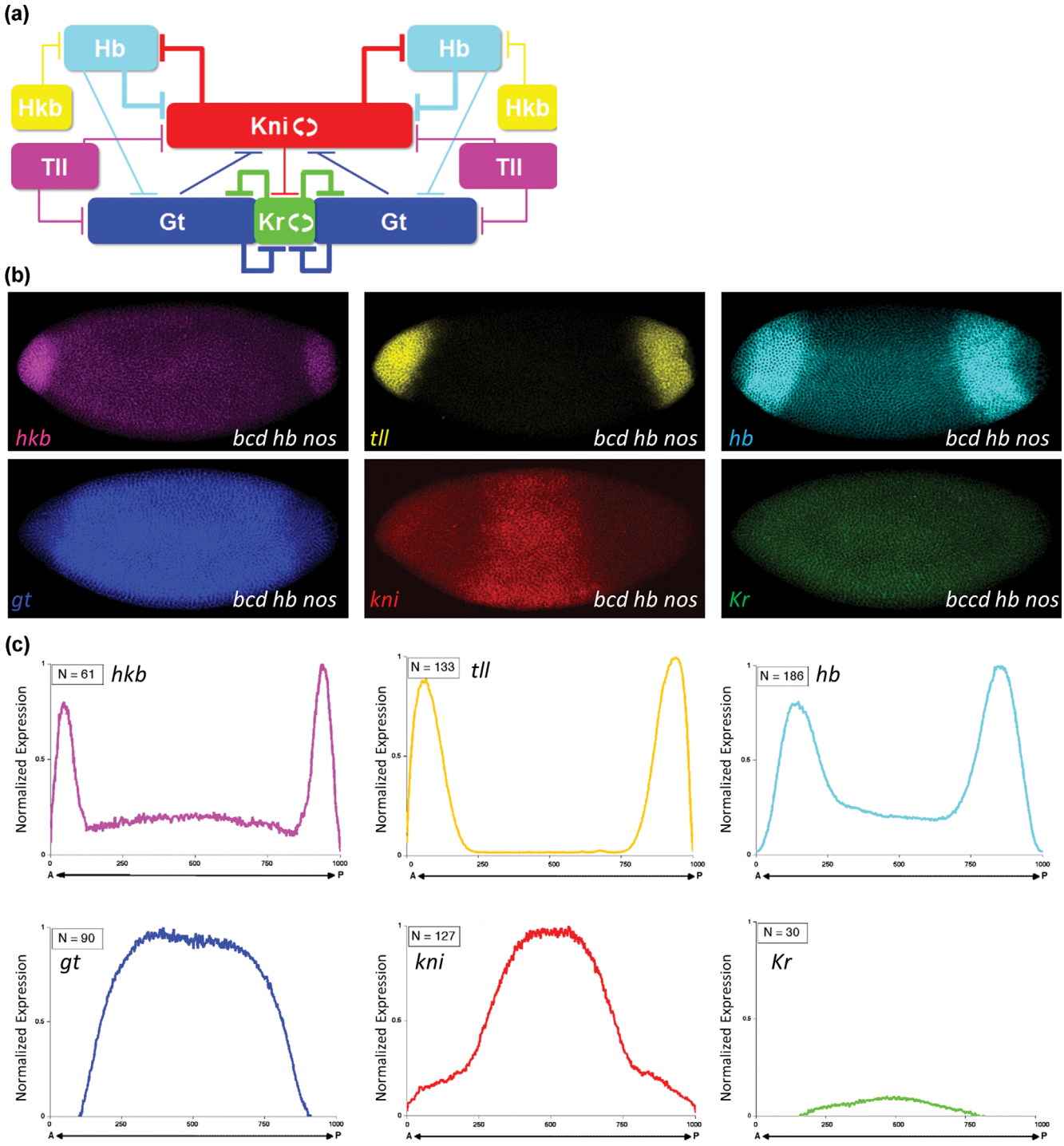

Fig. 3. Gap gene expression patterns in *bcd hb nos* germline clone embryos. (a) Schematic of the expression and regulatory model of the gap genes of *bcd hb nos* germline clone embryos. This model was derived based on the observed regulation of gap genes in wild-type embryos. (b) RNA-FISH images of the six gap genes in *bcd hb nos* embryos. (c) Quantified expression profiles of the gap genes in *bcd hb nos* mutant embryos. Average profiles are shown with the number of embryos indicated in each plot.

lapping patterns. Of note, in our analysis, we only compared the posterior half of the embryo as *bcd hb nos* mutant embryos showed duplication of the posterior structures in the anterior half.

We then visualized gap gene expression patterns in *bcd hb nos* germline clone embryos through RNA-FISH (Figs. 3(a) and 3(b)). Our prediction of the gap gene expression based on the previously reported regulatory interaction is shown in Fig. 3(a). We found that the posterior gene pattern is duplicated in the anterior half, which accounts for the duplication of the posterior structures in the anterior region of the cuticle (Fig. 1(h)). Overall, the expression pattern of the gap genes was similar to the ones we predicted. Notably, we found that *Kr* stripe was entirely missing in these embryos (Fig. 3(b)). Instead, *gt* and *kni* were expressed in overlapping patterns in the torso region where *Kr* was missing (Fig. 3(b)). This lack of *Kr* stripe could be explained by two possibilities: 1) Bcd is required to induce *Kr* transcription and/or 2) the shallow gradient of Cic might affect *gt* expression, which subsequently repressed *Kr*.

Going toward the poles from the torso region of the embryo, zygotic *hb*, *tll*, and *hkb* were detected. By quantifying the gene expression patterns, we could safely conclude that the terminal system alone could define the boundaries of zygotic *hb* and might be responsible for the lack of *Kr* expression. Moreover, as *hb* strongly represses the expression of *kni*, the terminal system could also define the boundary of *kni* and restrict the expression of *kni* to the torso region of the embryo.

As with the OreR embryos, the relationships between the gap genes can be elucidated by comparing quantified signal intensities (Fig. 3(c)). As in the OreR embryos, the strong mutual repression between *kni* and *hb* was observed. In addition, *hb* and *hkb* also showed weak repression. Interestingly, in this mutant embryo, *gt* and *hb* showed weak repression, which was consistent with the previous analysis of the gap gene network [23]. At the same time, the weak repressive relationship between *gt* and *kni* was still not observed in *bcd hb nos* embryos, as the two genes were expressed in overlapping patterns. Therefore, our data call for an adjustment

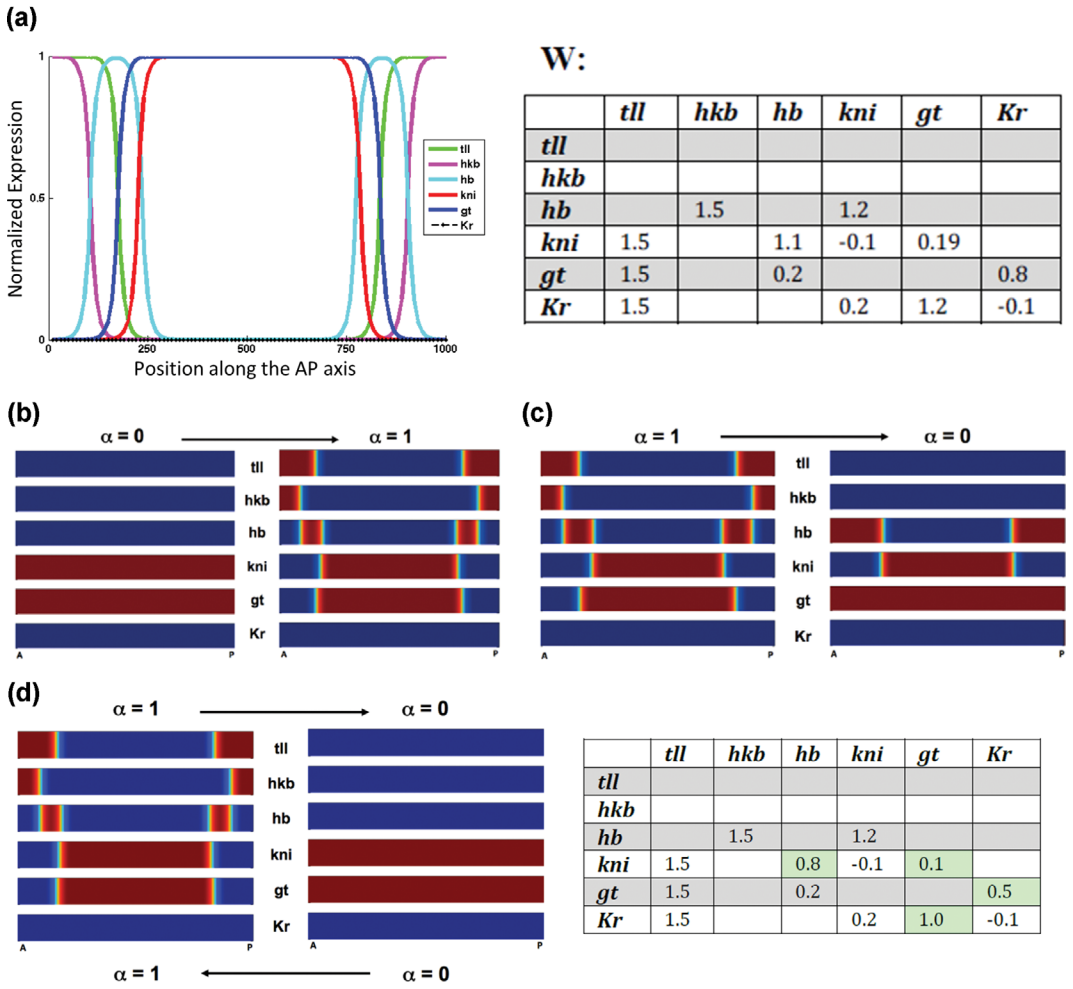

W:	tll	hkb	hb	kni	gt	Kr
tll						
hkb						
hb		1.5		1.2		
kni	1.5		1.1	-0.1	0.19	
gt	1.5		0.2			0.8
Kr	1.5			0.2	1.2	-0.1

	tll	hkb	hb	kni	gt	Kr
tll						
hkb						
hb		1.5		1.2		
kni	1.5		0.8	-0.1	0.1	
gt	1.5		0.2			0.5
Kr	1.5			0.2	1.0	-0.1

Fig. 4. Mathematical model of the gap gene regulation in *bcd hb nos* germline clone. (a) Prediction of the gap gene expression patterns by the reaction and diffusion model. The matrix of repressive weights used to generate such expression is shown on the right. The genes on the rows of the matrix were repressed by the genes on the columns. (b) Pcolor plot of gap gene expressions during the "on" dynamic of the MAPK signaling. (c) Pcolor plot of gap gene expressions during the "off" dynamic of the MAPK signaling. (d) Pcolor plot of gap gene expressions during on and off dynamic of the MAPK signaling for a monostable system. The matrix of repressive weights used to generate such expression is shown on the right. The genes on the rows of the matrix were repressed by the genes on the columns.

to the regulatory model of the gap gene network. We cannot exclude the possibility of *gt* regulating the posterior boundary of *kni* as proposed by previous studies [23,24]. However, our data clearly indicates that the relationship is more complex than simple weak repression.

3. Mathematical Modeling Reveals Potential Bistability in the Terminal System

To further analyze the gap gene pattern in *bcd hb nos* germline clones, we employed reaction and diffusion equations to model the gap gene network. Compared to wild-type embryos, *bcd hb nos* mutant embryos offer a simplified system with the terminal system having the sole spatial information. This mutant background affords an opportunity to test and predict parameters that describe the repressive relationship among the gap genes.

In our model, we used the Heaviside step function to describe gene transcription. We assumed that all the gap genes were activated by a uniform transcriptional activator, which was denoted by a positive term theta (θ). At the same time, gap genes were repressed by each other with repressive weights. Only when the θ term was greater than the repressive weights was the gene transcribed. To describe the effect of the terminal system, we quantified dpERK pattern from *bcd hb nos* embryos and fitted the data with the sum of two Gaussian curves. By doing so, we determined the parameter values to recapitulate the dpERK gradient, which was then used to calculate the spatial gradient of Cic with the Michaelis-Menten equation. The Cic gradient was used to model the repression for *tll* and *hkb*, the two terminal genes regulated by Cic. Lastly, we assumed that all gap gene mRNAs could diffuse with the same diffusivity and that they would undergo first-order degradation.

Our model prediction for the gap gene network in *bcd hb nos* embryos is shown in Fig. 4(a). According to our model, a repressive weight greater than one denotes strong repressive interaction, while 0.5 denotes weak interaction (Fig. 4(a)). In addition, negative weights represent autoregulation, which occurs for *Kr* and *kni*. After searching for the parameter set that recapitulates the experimental data, we found that two mutual repressive pairs (*hb-kni* and *gt-Kr*) were necessary. In addition, the repressive weights had to be similar, although not exact. Interestingly, the repressive weights of the terminal genes on other gap genes were very strong (Fig. 4(a)).

Using the developed model, we examined whether the terminal system could exhibit bistability in regulating gene expression patterns. To perform this test, the model was modified to include an alpha (α) term to describe the strength of the MAPK signaling with α=1 representing full activation and α=0 denoting the absence of the MAPK signaling. Starting with α=0, we slowly increased the term to 1 over 100 iterations using the results of each previous iteration as the initial condition for the next (Fig. 4(b)). Once the α value reached 1, we then re-started the iterations, but this time, decreasing α from 1 to 0 (Fig. 4(c)). We then asked whether the starting condition and the final condition resulted in the same gap gene expression patterns. We found that for certain sets of parameters, we could clearly observe that at α=0, the "off" dynamic (α from 1 to 0) generated a different expression pattern of *hb* and *kni* compared with that of the "on" dynamic (α from 0 to 1). This result indicates that the MAPK signaling system may work as a one-way switch in regulating *hb* and *kni* (Figs. 4(b) and 4(c)).

The existence of a bistable system implies that there might also be set parameters that generate a monostable system. By altering the parameters, but still requiring them to generate the correct gene expression pattern at α=1, a set was found that results in a monostable system (Fig. 4(d)). Therefore, parameter sets exist for which the system is single-valued and approaches the same result regardless of its starting point.

4. Maternal Hb can Regulate the Spatial Extent of the Terminal System

Previously, we showed that Hb protein could compete with Cic for access to dpERK and act as a competitive inhibitor of dpERK in the anterior region of the embryo [19,25,26]. Utilizing this effect of Hb, we examined embryos that lack *bcd* and *nos* but retain maternal *hb* expression to analyze the effect of uniformly deposited *hb* on the spatial extent of the terminal system. In this embryo, the terminal system was still the only maternal system with spatial information along the AP axis. We first analyzed the cuticle and found that these embryos also develop a symmetric pattern, but it is strikingly different from that of *bcd hb nos* germline clones (Fig. 5(a)).

We then analyzed the gap gene expression patterns in *bcd nos* embryos (Fig. 5(b)). Consistent with our expectation, the spatial extent of the MAPK signaling was restricted near the poles as the boundaries of *tll* and *hkb* were contracted. Interestingly, these embryos showed two stripes of *gt* rather than one large expression in the torso region, as in *bcd hb nos* embryos. In addition, the *Kr* stripe reappeared in the torso region of the embryo. The expression of *kni* was similar to that of *bcd hb nos,* but the size of the stripe became wider, most likely due to smaller zygotic *hb* expression.

Our analysis of *bcd nos* embryos provides insights toward understanding the missing *Kr* expression in *bcd hb nos* embryos. These two mutant embryos both lack Bcd protein, yet *Kr* expression is missing only in *bcd hb nos*. Therefore, although Bcd can activate *Kr* expression, Bcd is not essential. At the same time, decreased activity of dpERK allowed the activation of *Kr* transcription in the torso region of the embryo, as in *bcd nos* embryos. One possibility is the decreased zygotic *hb* stripe, which restricts the spatial extent of Hb protein to the poles. Consistent with this model, in *tor* gain-of-function mutant, *Kr* expression was mostly missing while zygotic *hb* was expressed in most of the torso region (Fig. 5(c)).

CONCLUSION

We examined the gap gene expression patterns in mutant embryos where the terminal system provides the sole source of spatial information along the AP axis, thus allowing for analysis of the spatial extent of the MAPK signaling pathway in patterning the early embryo. Our data clearly demonstrates that the terminal system works beyond the unsegmented termini and is sufficient to generate multiple segments along the AP axis of the embryo. Notably, the spatial extent of the MAPK signaling can influence the spatial boundaries of gap genes other than *tll* and *hkb*. Specifically, the expression of *Kr* in the torso region can be regulated by MAPK signaling. While *bcd hb nos* germline clone did not show any *Kr* expression, *bcd nos* mutant embryos with spatially uniform maternal Hb protein resulted in a broad expression of *Kr* in the torso

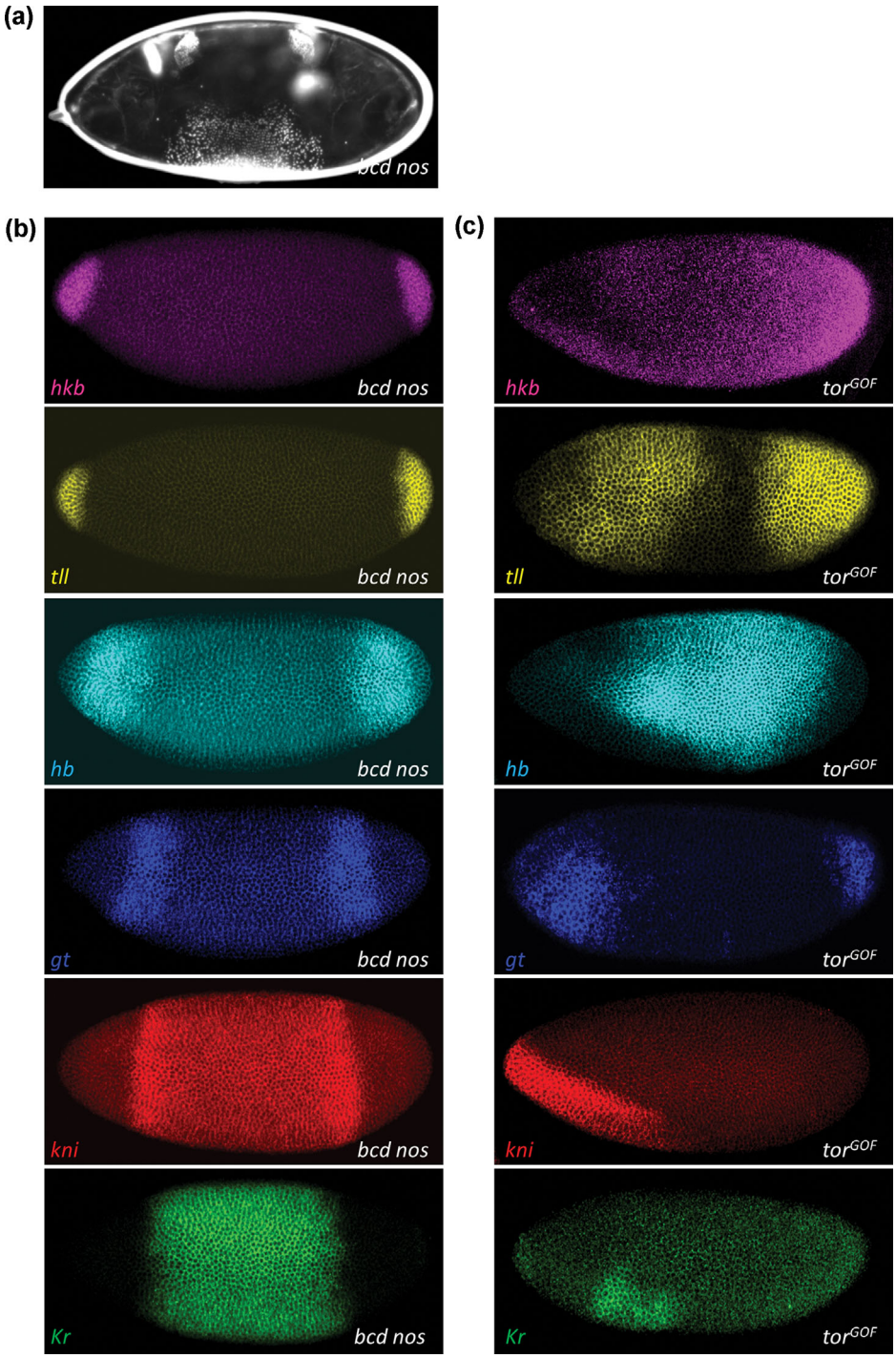

Fig. 5. Gap gene expression patterns in *bcd nos* and *tor* gain-of-function mutant embryos. (a) Embryonic cuticle produced by embryos lacking *bcd* and *nos* but retaining maternal *hb*. (b), (c) RNA-FISH images of the six gap genes in *bcd nos* (b) and Tor gain-of-function (GOF) (c) embryos.

region. This *Kr* expression affects the pattern of *gt*, which further alters the downstream segmentation process. Together, our analysis indicates that the repression of maternal *hb* translation by Nos in the posterior region might regulate the posterior boundary of *Kr* in wild-type embryos. Of note, our data cannot exclude the possibility where maternal Hb protein is directly responsible for the transcriptional activation of *Kr*. Indeed, previous studies showed that at low concentrations, Hb could activate gene expression [27]. Such possibilities should be tested in the future.

Our study provides insights into the regulation of the gap genes and suggests a potential function of maternal *hb* in regulating gap gene expression. Using the experimental data, we developed a mathematical model for the gap gene regulation that could recapitulate the wild-type and mutant data. Notably, our mathematical model

suggests the potential existence of bistability in the terminal patterning system. It would be interesting to analyze whether such bistability results in one-way switch behavior to maintain the stripe pattern of the gap genes even after the terminal signal shuts off. In conclusion, our study provides valuable resources in understanding the gene regulation by the MAPK signaling system in patterning complex tissues like early *Drosophila* embryos.

ACKNOWLEDGEMENTS

We thank Dr. Eric Wieschaus for providing *bcd hb nos* mutant flies and for the helpful discussions. K.M.O. was supported by thesis research funds by Princeton University. Y.K. was supported by the internal fund of Electronics and Telecommunications Research Institute (ETRI) [22RB1100, Exploratory and Strategic Research of ETRI-KAIST ICT Future Technology (Grant number: N05220126)].

AUTHOR CONTRIBUTION

K.M.O., S.Y.S., and Y.K. designed the experiments, K.M.O. and Y.K. performed the experiments. K.L., K.M.O., and J.K., performed image analysis. K.L., K.M.O., and Y.K. wrote the paper. All authors analyzed the data.

NOMENCLATURE

OreR : Oregon R
AP : Anteroposterior
Bcd : Bicoid
Hb : Hunchback
MAPK : Mitogen-activated protein kinase
ERK : Extracellular signal-regulated kinase
dpERK : Diphosphorylated ERK
Tor : Torso
Trk : Trunk
Tll : Tailless
Hkb : Huckebein
Cic : Capicua
Gro : Groucho
FISH : Fluorescent in situ hybridization
PBS : Phosphate-buffered saline
PBST : Phosphate buffered saline with 0.02% Triton X-100
DIG : Digoxigenin
BIO : Biotin
FITC : Fluorescein
WBR : Western blocking reagent
BSA : Bovine serum albumin
NGS : Normal goat serum
Kr : Krüppel
Kni : Knirps
Gt : Giant
GOF : Gain-of-function

REFERENCE

1. J. Jaeger, Manu and J. Reinitz, *Curr. Opin Genet. Dev.*, **22**, 533 (2012).
2. E. Wieschaus, *Curr. Top Dev. Biol.*, **117**, 567 (2016).
3. J. Casanova and G. Struhl, *Genes Dev.*, **3**, 2025 (1989).
4. W. Driever and C. Nusslein-Volhard, *Cell*, **54**, 95 (1988).
5. J. Jaeger, *Cell Mol. Life Sci.*, **68**, 243 (2011).
6. D. St Johnston and C. Nusslein-Volhard, *Cell*, **68**, 201 (1992).
7. M. Akam, *Development*, **101**, 1 (1987).
8. A. Ephrussi and D. St Johnston, *Cell*, **116**, 143 (2004).
9. J. Dubnau and G. Struhl, *Nature*, **379**, 694 (1996).
10. R. Rivera-Pomar, D. Niessing, U. Schmidt-Ott, W. J. Gehring and H. Jackle, *Nature*, **379**, 746 (1996).
11. E. De Keuckelaere, P. Hulpiau, Y. Saeys, G. Berx and F. van Roy, *Cell Mol. Life Sci.*, **75**, 1929 (2018).
12. R. Lehmann and C. Nusslein-Volhard, *Development*, **112**, 679 (1991).
13. C. Wreden, A. C. Verrotti, J. A. Schisa, M. E. Lieberfarb and S. Strickland, *Development*, **124**, 3015 (1997).
14. M. Furriols and J. Casanova, *Embo J.*, **22**, 1947 (2003).
15. C. M. Smits and S. Y. Shvartsman, *Curr. Top Dev. Biol.*, **137**, 193 (2020).
16. A. Mineo, M. Furriols and J. Casanova, *Open Biol*, **8**, 180180 (2018).
17. E. Cinnamon, A. Helman, R. Ben-Haroush Schyr, A. Orian, G. Jimenez and Z. Paroush, *Development*, **135**, 829 (2008).
18. G. Jimenez, A. Guichet, A. Ephrussi and J. Casanova, *Genes Dev.*, **14**, 224 (2000).
19. Y. Kim, M. Coppey, R. Grossman, L. Ajuria, G. Jimenez, Z. Paroush and S. Y. Shvartsman, *Curr. Biol.*, **20**, 446 (2010).
20. H. E. Johnson, Y. Goyal, N. L. Pannucci, T. Schupbach, S. Y. Shvartsman and J. E. Toettcher, *Dev. Cell*, **40**, 185 (2017).
21. M. Coppey, A. N. Boettiger, A. M. Berezhkovskii and S. Y. Shvartsman, *Curr. Biol.*, **18**, 915 (2008).
22. Y. Kim, A. Iagovitina, K. Ishihara, K. M. Fitzgerald, B. Deplancke, D. Papatsenko and S. Y. Shvartsman, *Chaos*, **23**, 025105 (2013).
23. M. Ashyraliyev, K. Siggens, H. Janssens, J. Blom, A. Akam and J. Jaeger, *PLoS Comput. Biol.*, **5**, e1000548 (2009).
24. T. J. Perkins, J. Jaeger, J. Reinitz and L. Glass, *PLoS Comput. Biol.*, **2**, e51 (2006).
25. Y. Kim, M. J. Andreu, B. Lim, K. Chung, M. Terayama, G. Jimenez, C. A. Berg, H. Lu and S. Y. Shvartsman, *Dev. Cell*, **20**, 880 (2011).
26. Y. Kim, Z. Paroush, K. Nairz, E. Hafen, G. Jimenez and S. Y. Shvartsman, *Mol. Syst. Biol.*, **7**, 467 (2011).
27. D. Papatsenko and M. S. Levine, *Proc. Natl. Acad Sci. USA*, **105**, 2901 (2008).